Chapter 3

Synthesis and characterization of dispersions of $ZnCrO_4$ prepared in AOT stabilized water/heptane microemulsion

Abstract

This chapter gives a description of the synthesis of zinc chromate ($ZnCrO_4$) NP in microemulsion medium has been stated. The microemulsion composed of H_2O/AOT (sodium bis(2-ethylhexylsulfosuccinate))/ n-heptane water-in-oil (W/O) is used to prepare the $ZnCrO_4$ dispersion. Various parameters such as water pool sizes, precursor concentration and sonication are considered to tune the size of the NPs. The formation of $ZnCrO_4$ in the microemulsion has been verified by XRD and FTIR measurements. The absorbance of the dispersions formed in different water pool sizes was studied. Their dimension in the microemulsion medium is determined by the dynamic light scattering method. Enthalpy of formation of $ZnCrO_4$ in W/O microemulsion medium is measured by isothermal titration calorimetry (ITC). The dimension and morphology of the formed $ZnCrO_4$ colloidal particles examined by transmission electron microscopy (TEM) are strongly dependent on the water pool size, precursor concentration and sonication.

3.1. Introduction

In general, a particle is defined as a small and stable object that possesses characteristic physicochemical properties. It is classified according to its particle size.[1] Fine particles cover a range between 100 and 2500 nm, while ultra fine particles or nanoparticles are sized between 1 and 100 nm. Nanoparticles normally exhibit size-regulated properties that significantly differ from those of fine particles or bulk.[2-13] In agglomerating bodies formed from nanoparticles, irregular particle size and morphology often lead to non-uniform packing characteristics, *viz.*, density, resistivity, dielectric constant, etc. Difficult-to-control agglomeration of nanoparticles under an influence of vander Waals force of attraction can result in microstructural inhomogeneity. There are thus requirements of novel processes for the preparation of uniform nanoparticles (with less agglomeration) to avoid inconsistencies in the synthesized products. A uniformly dispersed assembly of strongly interacting nanoparticles in suspension requires total control over their interacting forces. Production of monodisperse nanoparticles by microemulsion process is well recognized as a potential mean for industrial applications.[14]

Among various methods to prepare nanoparticles, in particular, the nanoscale water pool compartment within the water-in-oil (W/O) microemulsion is an effective and inexpensive template due to operation under mild conditions. [6 ,7, 10, 15-19] Many difficulties in the preparation of nanoparticles by other methods can be overcome by the use of microemulsion. The dispersed waterpool behave as microreactor in which chemical reaction can be performed to generate the desirable product in a form of colloidal dispersion of desired sizes in the nanometer scale.[20-23] In this process, size of the nanoparticles can be controlled; therefore, monodispersity and prolonged stability can be favourably achieved.[19,24] As a result, the synthesized nanoparticles exhibit optical, magnetic, and structural properties which are absent in bulk condition.[25-29]

Regarding to a variety of novel nanoparticulate dyes, $ZnCrO_4$ or zinc yellow has been for long recognized as a very useful dye/pigment. In addition, it has been widely used as, corrosion inhibitor and a good catalyst.[30-35] It is expected that the above mentioned properties of the $ZnCrO_4$ may undergo changes due to size reduction in the nanometer scale.

The present manuscript describes the synthesis and characterization of nano dispersions of $ZnCrO_4$ prepared in the water pool of water-in-oil (W/O) microemulsion comprising water/AOT/n-heptane. The prepared $ZnCrO_4$ nanoparticles were characterized to confirm their chemical constitutions by XRD, EDS and FTIR spectroscopy. Physicochemical properties of the nanoparticles were evaluated by UV-vis absorption spectroscopy, dynamic light scattering (DLS), transmission electron microscopy (TEM) and isothermal titration calorimetry (ITC).

3.2. Experimental

3.2.1. Materials

Sodium *bis*(2-ethylhexyl)sulfosuccinate, commonly known as AOT, was a 99% pure product of Acros Organic (USA). Spectroscopic grade n-heptane and acetone were purchased from S.D. Fine Chem. Ltd. (India). AR grade zinc sulfate heptahydrate and potassium chromate were products of E. Merck (India). Doubly distilled water was used in the preparation of aqueous solutions.

3.2.2 Methods

3.2.2.1 Synthesis of $ZnCrO_4$

At different [water]/[AOT] molar ratio (ω), a W/O microemulsion containing precursor K_2CrO_4 and another containing precursor $ZnSO_4$ were separately prepared. The precursor concentrations were varied in the range of 0.1 to 0.4 mol dm^{-3} where the template (microemulsion) was found to be stable.[36,37] In a typical experiment, the microemulsion containing K_2CrO_4 was added drop wise into the microemulsion of $ZnSO_4$ under gentle stirring up to stoichiometric requirement. The stable microemulsions containing the orange yellow $ZnCrO_4$ suspension with a specific concentration were obtained by varying $[H_2O]/[AOT]$ (ω) in the range of 2, 5, 10, 15 and 20. The prepared materials in the microemulsions were aged for a week in prior to their physicochemical characterization.

3.2.2.2. Isolation of nanoparticles from microemulsion

The colloidal nanodipersion of $ZnCrO_4$ in W/O microemulsion was treated with excess acetone to stimulate instability of microemulsion and precipitation of solid $ZnCrO_4$ particles settling down to the bottom of the vessel.[22,23,36] The precipitate was then decanted and washed several times with acetone, n heptane and water to remove the residual components, *viz*., K_2SO_4, AOT, K_2CrO_4 and $ZnSO_4$. The $ZnCrO_4$ particles were then dried in an oven to remove the remaining acetone, producing orange yellow powder which was subjected to various characterization.[37,38]

3.2.3. Instrumentation

Powder X-ray diffraction (XRD) analyses were taken by a Bruker Model D8 Advance diffractometer (Bruker, Germany). Fourier transform infrared (FT-IR) spectroscopic measurements were conducted using a Shimadzu 8300 instrument (Shimadzu, Japan). The precursors and isolated $ZnCrO_4$ were mixed separately with KBr and converted into pellets by compressing with a pressure of 780 MPa. The spectra were recorded for 34 times to get the final results and compared with literature reported values.[39] UV-visible spectra were taken in a Spectro UV-vis double beam PC scanning spectrophotometer, UVD-2950 (LABOMED, USA), using quartz cuvette of optical path length of 1.0 cm. The hydrodynamic diameters of colloidal particles of $ZnCrO_4$, embedded in H_2O/AOT/n-heptane W/O microemulsion media were measured in a dynamic light scattering spectrophotometer (DLS-ZETA SIZER NANO Z-S90, Malvern Instrument, U.K.). All measurements were taken at a fixed angle of 90º. Samples were filtered several timed through 0.24 μm millipore membrane filters in prior to all measurements. The intensity data from DLS was modified to obtain hydrodynamic diameter (d_h), polydispersity index (PDI), and diffusion co-efficient (D) of the AOT-coated colloidal $ZnCrO_4$ particles in the microemulsion medium.[37,40,41] Transmission electron microscopic analysis of $ZnCrO_4$ nanoparticles was also conducted using JEM 2100 transmission electron microscope (JEOL, Japan). Carbon coated copper grid was used for such measurements. A drop of nanocolloidal dispersions of zinc chromate was dropped on the grid and it was then was dried at room temperature for 30 min and then used.

Enthalpies of the reaction between $ZnSO_4$ and K_2CrO_4 in both aqueous and microemulsion media were measured in an isothermal titration microcalorimeter (Microcal, USA). 1.325 mL of $ZnSO_4$ suspension was taken in the measuring cell. Then 300 μL of the chromate solution was stepwise injected in the cell in 30 installments with constant stirring (350 rpm) condition. The thermal history of the mixture was recorded and processed using the software after subtracting the enthalpy of dilution of K_2CrO_4 (measured by diluting the K_2CrO_4 microemulsion solution into the microemulsion containing only water). In all the cases, excessive $ZnSO_4$ solution was introduced into the microemulsion in order to ensure the complete formation of $ZnCrO_4$.[37,40,41] All measurements except XRD, TEM, were taken at 303+0.01K

3.3 Results and discussion

3 3.1. XRD analysis

The characterization of isolated $ZnCrO_4$ nanoparticles at ω=15 was made by XRD methods. By computer analysis the XRD data, *i.e.*, the diffraction pattern, the angle of reflection, and intensities were obtained as illustrated in figure 3.1A. The diffraction patterns were compared with the standard reference file for confirmation of peaks at 19, 21, 32, 35, 52, 54 and 73º which correspond to the diffraction pattern of chromate nanocrystals.[38,42,43] It should be noted that no significant shift in the diffraction angle was observed in our analyses of all $ZnCrO_4$ nanoparticles synthesized at different precursor concentration and different [water]/[AOT] molar ratio (ω). Based on the analysis, it is confirmed that the XRD peaks shown in Figure 3.1 are consistent with others previous works of zinc chromate nano crystals synthesised in different way.[42,44]

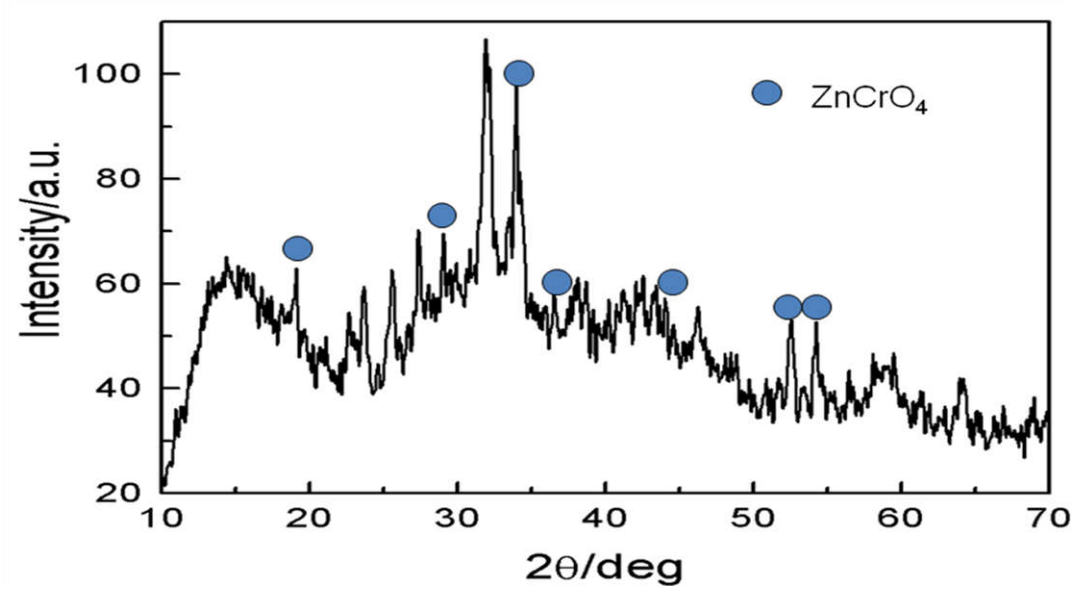

Figure 3.1. A. X-ray diffraction pattern of zinc chromate particles prepared in water/AOT/n-heptane microemulsion.

3.3.2. FT-IR spectra analysis

Figure 3.1.B shows the FTIR spectra of the isolated aggregates of $ZnCrO_4$, alongwith the spectra of K_2CrO_4 and $ZnCrO_4$ synthesized in bulk water. Table S3.1 also summarizes the FTIR analytical results of K_2CrO_4 and $ZnCrO_4$ synthesized by the primitive bulk reaction and microemulsion routes. While pure K_2CrO_4 showed a single peak at 882 cm^{-1} alongwith a faint peak at 719 cm^{-1}, the $ZnCrO_4$ synthesized by the bulk reaction route exhibited three distinctive peaks at 719, 879 and 955 cm^{-1}. The characteristic peaks of the $ZnCrO_4$ synthesized by the microemulsion route at different ω values were found to vary from 890 cm^{-1} to 928 cm^{-1}. As ω values increased, distinct blue shifts in the relevant peaks were noticed. From ω_{20} to ω_{15}, ω_{15} to ω_{10}, ω_{10} to ω_5 the shifts are 6, 3 and 29 cm^{-1} respectively. However another peak increment in the range 719 cm^{-1} to 723 cm^{-1} shows the weak peak indication of $ZnCrO_4$. According to Nakamoto et al. the spectrum of $[CrO_4]^{2-}$ anion should have fundamental frequencies at $\upsilon_1 = 833$, $\upsilon_2 = 339$, $\upsilon_3 = 863$ and $\upsilon_4 = 375$ cm^{-1} (of which υ_1 and υ_3 are IR active).[45, 46] The IR spectroscopy of $ZnCrO_4$ show that 772 cm^{-1} is weak, 872 cm^{-1} is strong, 892 cm^{-1} is medium, 941 cm^{-1} is medium peak indication of of $ZnCrO_4$ sample.[44] FTIR signal shift of $ZnCrO_4$ nanoparticles was ascribed to the

size confinement effect resulted from the nano scaled characteristics of the synthesized products. In particular, the intensities of vibrational bands of IR spectra decrease to the inverse of crystallite size. It was shown that the spectra demonstrated a significant dependence on the size of the crystallites.[47] Formation of nanoparticles of $ZnCrO_4$ is, therefore, confirmed.

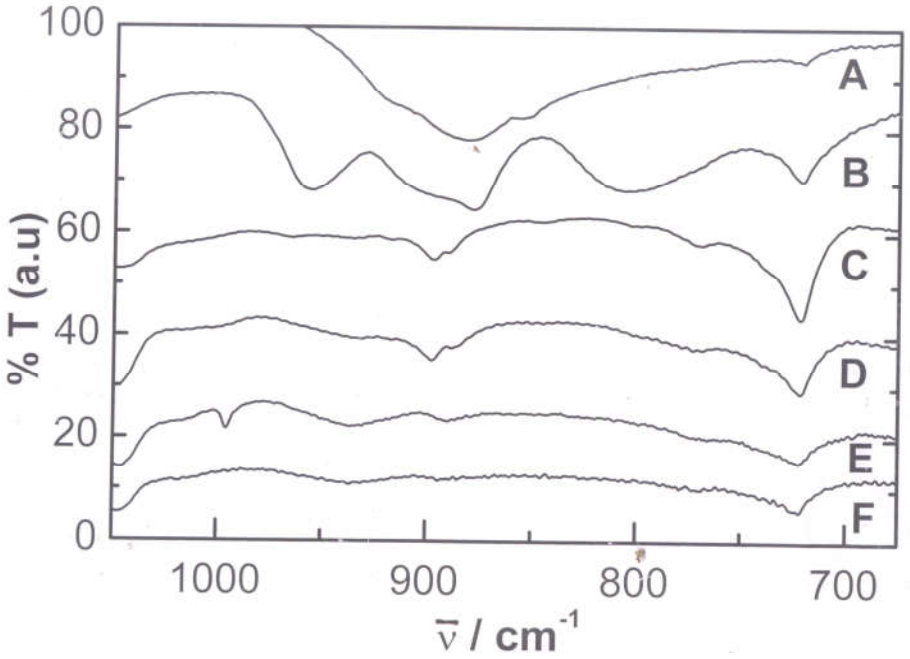

Figure 3.1.B. FTIR spectra of K_2CrO_4 (A); $ZnCrO_4$ prepared in bulk water (B) and in water/AOT/n-heptane W/O microemulsion at ω = 20 (C); 15(D); 10 (E) and 5 (F).

3.3.3. Absorption spectra analysis

The visible spectra of colloidal suspensions of $ZnCrO_4$ with four different concentrations are depicted in Figure 3.2. In this figure, intensity of absorbance increased with concentration. This fact is similar for $K2CrO_4$, which is shown in the inset of Figure 3.2. At a designated ω, the absorbance at 273 and 370 nm increased linearly with respect to the increase in the concentration of $ZnCrO_4$. The synthesized $ZnCrO_4$ suspension behaved like normal suspension obeying Beer's law similar to those results reported on other encapsulated microemulsions, such as copper ferrocyanide, [37] lead chromate[38] and other copper salts.

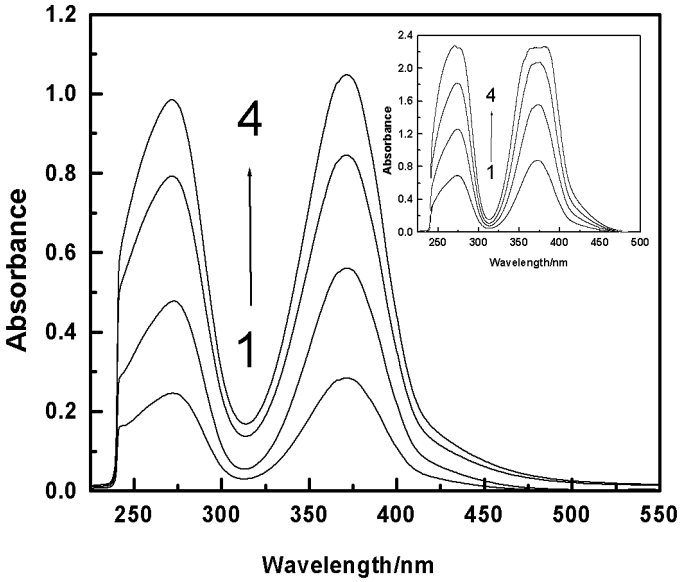

Figure 3.2 Absorption spectra of colloidal $ZnCrO_4$ in water/AOT/heptane W/O microemulsion at 303K at ω = 15. Overall concentration of complex/mmoldm^3: 1, 0.10; 2, 0.35; 3, 0.53 and 4, 0.71. Inset: absorption spectra of K_2CrO_4 at ω = 15. Overall concentration of K_2CrO_4 /mmoldm^3: 1, 0.2; 2, 0.7; 3, 1.06 and 4, 1.42.

Similarly the spectra of $ZnCrO_4$ nanoparticles at a designated concentration of $5.3x10^{-4}$ mol dm^{-3} with various ω (2, 5, 10, 15 and 20) are also illustrated in Figure 3.3.

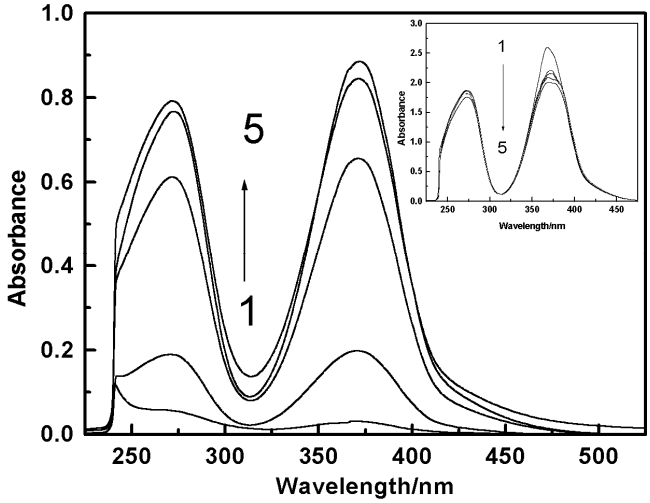

Figure 3.3 Absorption spectra of colloidal zinc chromate ($5.3x10^{-4}$ mol dm^{-3}) prepared in H_2O/AOT/n-heptane W/O microemulsion at different ω values at 303K. Curves 1-5: ω values 2, 5, 10, 15 and 20. Inset: absorption spectra of K_2CrO_4 ($1.0x10^{-4}$ mol dm^{-3}) in the same medium at various ω values.

It can be noticed from Figure 3.2 and Figure 3.3 that there are two maxima at 273 and 370 nm. The absorbance intensity became higher with the increase in ω, resulted from the increase in ZnCrO4 particle size. With the increase of size of the droplets of microemulsion, the transmitance decrease and absorbance increase. This fact is established from the molar absorption coefficient values at different ω, shown in Table S3.2. Also as the particle size of $ZnCrO_4$ increase the scattering property decrease and absorption increase. Due to these facts the intensity of absorbance increased with the increase in ω. In the inset of Figure 3.3 the spectra of K_2CrO_4 at concentration of $1.0x10^{-4}$ mol dm^{-3} with varied ω values are also shown. However, the absorbance intensity decreased with the increase in ω value due to the dilution effect of the aqueous water pool.[37, 38, 43] Although the absorption peaks of $ZnCrO_4$ in microemulsion medium are identical to those of K_2CrO_4, but their absorbance ranges are different. The absorbance of K_2CrO_4, in solution, is higher than that of $ZnCrO_4$, as the nanoparticles in microemulsion have relatively lower electronic transitions. The absorbance at both 273 and 370 nm was enhanced almost linearly with the increase in ω value up to 12, then tended to level out with the further increase in ω (Figure 3.4).

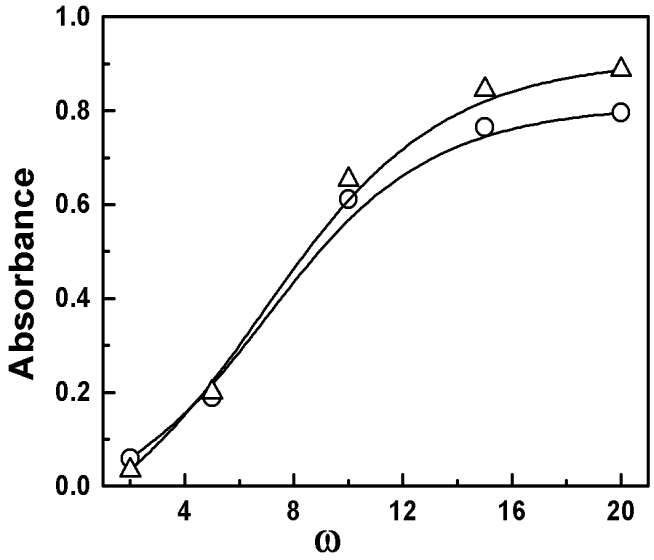

Figure 3.4 Variation of absorbance (O, at 273nm and , at 370 nm) with ω for the nanocolloidal dispersion of $ZnCrO_4$ prepared in water/AOT/n-heptane W/O microemulsion.

With the increasing particle size the $ZnCrO_4$ suspension gradually lost its transparency, which was linear initially up to ω = 12. Based on all linear plots, the molar absorbance coefficients of $ZnCrO_4$ nanoparticles at different wavelength as well as at different ω values were evaluated. It should be noted that the visible spectral data were processed in terms of the following equation to obtain the value of band gap (ε_g) of the $ZnCrO_4$ nanoparticles encapsulated in the microemulsion medium.[48, 49]

$$(\varepsilon h\nu)^2 = C(h\nu-\varepsilon_g) \qquad (3.1)$$

Where, ε, h, and ν are the molar absorption co-efficient, Planck's constant and frequency of light respectively and C is a constant.

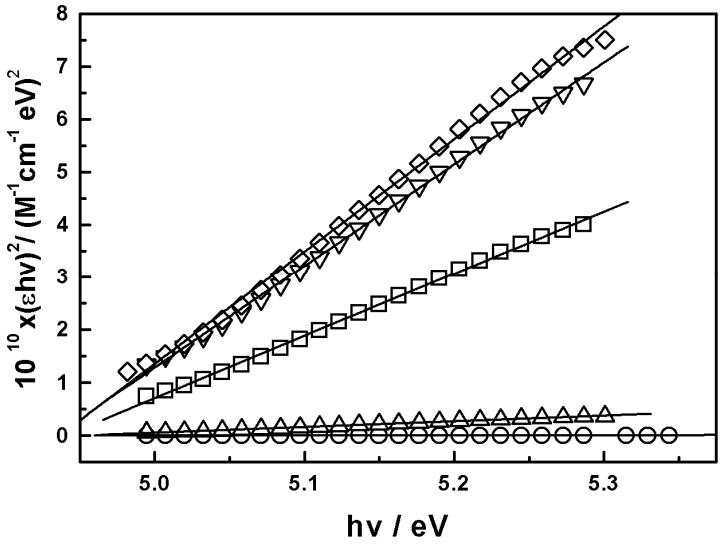

Figure 3.5 Plot of $(\varepsilon h\nu)^2$ against hν at fixed concentration of $ZnCrO_4$ ($5.3x10^{-4}$ mol dm^{-3}) with various ω values. The symbols O, , □, □ and display the values of increasing ω = 2, 5, 10, 15, 20 respectively

Figure 3.5 describes the variation of $(\varepsilon h\nu)^2$ at different hν values. The variations were found to be linear and the band gap values were calculated from the ratio of the intercept and the slope according to equation 3.1. In this evaluation, absorbance values corresponding to longer wavelength sides were taken into account since the lights of shorter wavelengths might cause transmission of electrons to energy levels higher than the band gap.[50] The average ε_g value has been found to be 3.01.eV, which was found to be comparable with the previously obtained values for other nanoparticles containing chromate anions. The band gap, in the present case, lies in the region corresponding to the normal semiconductor materials.

3.3.4. DLS study

In the present study, hydrodynamic diameter of the $ZnCrO_4$ nanoparticles prepared in water/AOT/n-heptane W/O microemulsion medium under different conditions (varying ω and concentration) were determined. Also to compare the related results for nanoparticles, the DLS analyses were performed with the precursor loaded and bare (containing water only) microemulsions. By applying the equation of Paul and Moulik [51] the d_h values were evaluated:

$$d_h = 2\,(1.185 + 0.13\omega) \qquad (3.2)$$

Figure 3.6 summarizes the results on the DLS studies on different microemulsions as mentioned above.

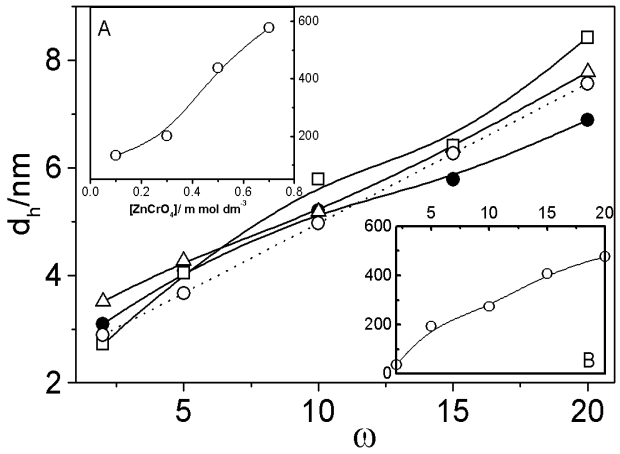

Figure 3.6. Profile of d_h/nm vs ω. The symbols ○, ●, □ and represent the values of d_h of microemulsion droplets containing water, K_2CrO_4 (0.6 mmol dm^{-3}), $ZnSO_4$ (0.6 mmol dm^{-3}), and theoretical values (according to Moulik et al., ref. 51) respectively. Inset: (A) Variation of d_h with the concentration of $ZnCrO_4$ in microemulsion medium at ω= 5. (B) d_h (nm) profile for a 0.3 mmol dm^{-3} $ZnCrO_4$ in microemulsion medium.

According to Ray et al.[52] d_h is expected to vary linearly with ω. With the increased ω, size of the $ZnCrO_4$ nanoparticles also became larger, shown in inset (B) of Figure 3.6 Similarly, with the increase in concentration of $ZnCrO_4$ the d_h value also increased as could be confirmed by results shown in the inset (A) of Figure 3.6. In earlier studies,[37,38] the variation of d_h with ω follows a positive deviation from the calculated values (equation 3.2). The $ZnCrO_4$ nanoparticles synthesized in H_2O/AOT/heptane system exhibited a higher d_h values ~100 nm, when compared with that of the theoretically calculated values. The observed values for bare microemulsion droplets exhibit a higher profile with ω when compared with that of the precursor or water loaded microemulsions (<10 nm). This phenomenon could be attributed to the size constriction

effect. The comparison of theoretical d_h values, d_h values of bare microemulsion and $ZnCrO_4$ loaded microemulsion are reported in Table 3.1

Table 3.1 Transmission Electron Microscopic (TEM) and DLS Results of Colloidal Zinc Chromate prepared in H_2O/AOT/n-heptane W/O Microemulsion (μE).

		TEM		Diameter (nm), obtained from DLS measurements		
	ω	Shape	Size/nm	Theoretical*	Bare μE	$ZnCrO_4$ loaded μE
Nonsonicated	2	No defined shape	100	2.89	2.50	74
	5	Aggregated	100	3.67	3.97	388
	10	Spherical(aggregated)	100	4.97	5.20	547
	15	Crystalline needle	200	6.27	7.0	815
	20	Spherical	200	7.57	8.1	953
Sonicated	2	Crystalline needle	100	2.89	1.7	70
	5	Crystalline needle	100	3.67	2.3	200
	10	Spherical	500	4.97	4.9	275
	15	Crystalline needle	200	6.27	6.1	410
	20	Crystalline	200	7.57	7.0	495

* According to Moulik's formalism (ref. 51)

The values of d_h of $ZnCrO_4$ are much more higher than theoretical, bare and precursors loaded microemulsions. This happened due to uncontrolled growth of $ZnCrO_4$ nanocrystals. Similar to the experience of previous reports, [38, 43] with a higher ω, the colloidal particles were found to be larger than expected size because the decrease in surface density of the stabilizer (AOT) would result in the unstable droplets as a consequence of enlargement due to aggregation. From the DLS measurements the ratio σ/d_h, where σ standing for a standard error in d_h, which is called as polydispersity index (PDI), could be determined. [37, 38, 40, 41, 53-56] The PDI value is 0.1 for monodispersed system. In an acceptable agreement with other results, [37, 38, 40, 41] the PDI values are higher than 0.1, suggesting that the $ZnCrO_4$ suspensions were fairly polydispersed.

3.3.5. Enthalpy of $ZnCrO_4$ formation

Dispersions of $ZnCrO_4$ nanoparticles were formed by the reaction between $ZnSO_4$ and K_2CrO_4 using W/O microemulsion template. The enthalpy of formation of $ZnCrO_4$ (H_f) was determined by the ITC method. [37, 38, 40, 41] The overall process appears to be exothermic in nature. With the increase in the ω value, the process became less exothermic. A typical H_f - ω profile is been shown in Figure 3.7.

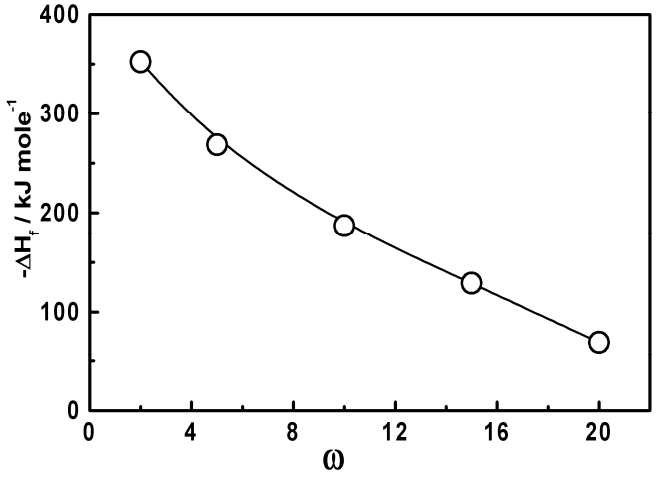

Figure 3.7 Plot of H_f vs. ω for the formation of $ZnCrO_4$ in H_2O/AOT/heptane W/O microemulsion at 303 K.

Evaluation of enthalpy of formation of the $ZnCrO_4$ suspension in the water pool of W/O microemulsion is not very common in literature.[37,41] During the self assembling reaction, mass exchange between $ZnSO_4$ and K_2CrO_4 containing water pools would take place and dominate the conversion of the reactants to form the $ZnCrO_4$ nanoparticles. Values of the enthalpy of formation at different water pool size in the microemulsion were found to be comparable with our previously reported results.[37,41] The enthalpy of formation of both the nanoparticle suspensions of copper ferrocyanide and tungstic acid in the water pool of W/O microemulsion were found to vary linearly with the reciprocal of ω. The variation of enthalpy of $ZnCrO_4$ formation with ω decreased exponentially which differs from the case of copper ferrocyanide. This is due to the difference in morphology of copper ferrocyanide and $ZnCrO_4$. Copper

ferrocyanide is gelatine in nature, so the growth of the nano copper ferrocyanide can be controlled, but as $ZnCrO_4$ is crystalline, growth of formation become uncontrolled at higher ω, so the curve becomes exponential. The different environmental factors would also be expected to influence the energetics of the process. The resultant enthalpy of formation of the nanoparticle suspensions in W/O microemulsion is a resultant effect of the different processes, viz., droplet fusion, mass exchange, product formation, droplet fission and molecular reorganization of the formed product. With the increase in size of the water pool in the microemulsion, it is expected to get larger colloidal nanoparticles, which requires some additional heat for the process of nucleation.

3.3.6. Electron microscopic analysis

The transmission electron microscopic (TEM) measurements were carried out for analyzing the $ZnCrO_4$ nanoparticles of (ω = 2, 10, 20) synthesized with and without the sonicating conditions. The results are summarized in Table 3.1. Some representative micrographs of TEM are shown in Figures 3.8 and 3.9.

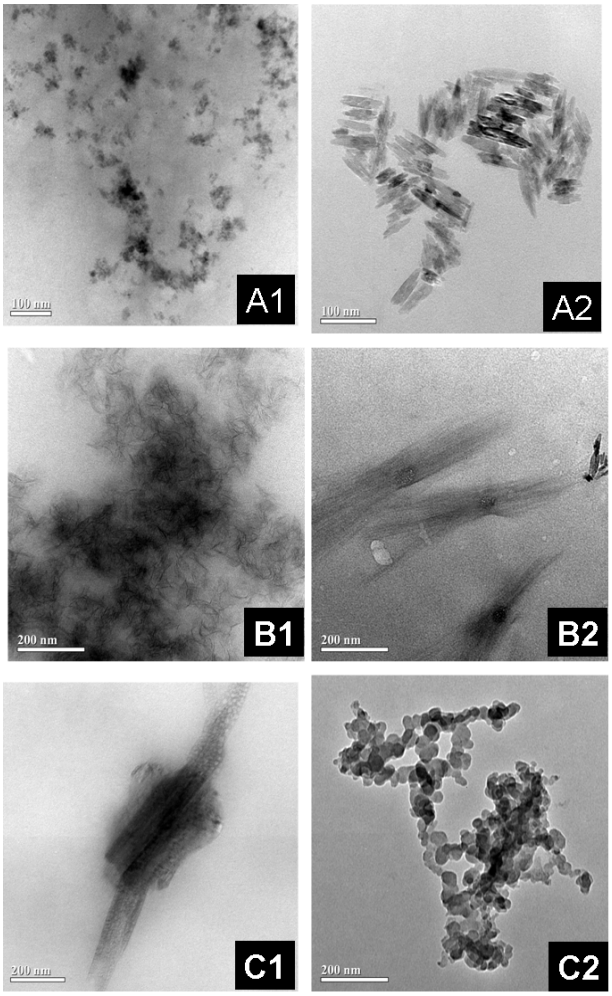

Figure 3.8 Transmission electron micrograph of colloidal $ZnCrO_4$ dispersions prepared in water/AOT/n-heptane W/O microemulsion at [water]/[AOT] mole ratio, ω = 2 (A), 10(B) and 20 (C) 1, nonsonicated, 2, sonicated. Scale bar: (A) 100 nm, (B) and (C), 200 nm.

The micrographs of unsonicated samples show an irregular morphology while the corresponding sonicated samples exhibits their distinct shapes. It is expected that in the absence of sonication the irregular growth of the $ZnCrO_4$ nanoparticles would be more dominated. On the other hand, sonication could lead to the formation of smaller nanoparticles with well organized morphology. The electron microscopic data also supported this postulation. Overall dimension of the $ZnCrO_4$ nanoparticles was found to increase with the increase in ω value.[37,38,41,]

[55] This observation further supports the results obtained by DLS method. The synthesized $ZnCrO_4$ nanoparticles mostly exist in needle-like shape. However, at ω = 20, the sonicated sample yielded fractal-like structures. Regarding the advantage of nanoparticle synthesis using water in oil microemulsion template, the size and shape of the dispersed nanoparticles could be controlled. With the increased water pool size it is common to expect bigger particles. However, it is also known that above ω~15, the water pool in the microemulsion behaved like bulk water, resulting in the formation of fractal-like structures.[37, 38, 57, 58] In such fractal structure, smaller aggregates were formed then grow further through the continuous emergence of nucleate nanostructures.[37]

Effect of concentration on the shape of the synthesized $ZnCrO_4$ nanoparticles was also found to be significant. The increased concentration of the precursor led to the increase in the amorphous nature of the synthesized nanoparticles, consequently resulting in the irregular morphology of the nanoparticles. At the same size of the water pool, if the concentration of the formed product was increased, then the number of stabilizing agent (herein the surfactant, AOT) per cluster would oppositely decrease. As a consequence, the formation of $ZnCrO_4$ nanoparticles with larger heterogeneity would take place. Though the morphology the samples subjected to TEM analysis is different, it is still under investigation that the sample A2 with longer aspect would have significantly higher crystallinity than others. The dimension of $ZnCrO_4$ nanoparticles obtained in DLS was found to be higher when compared with TEM results. The DLS dimensions were analyzed based on a postulation of spherical particles moving in solution whereas the TEM findings take into account of visible geometric appearance of each individual nanoparticle. Therefore, both results would not provide the same absolute dimension values hut it should be noted that ω = 10 fairly agreed with each other because of the spherical morphology of the synthesized $ZnCrO_4$ nanoparticles.

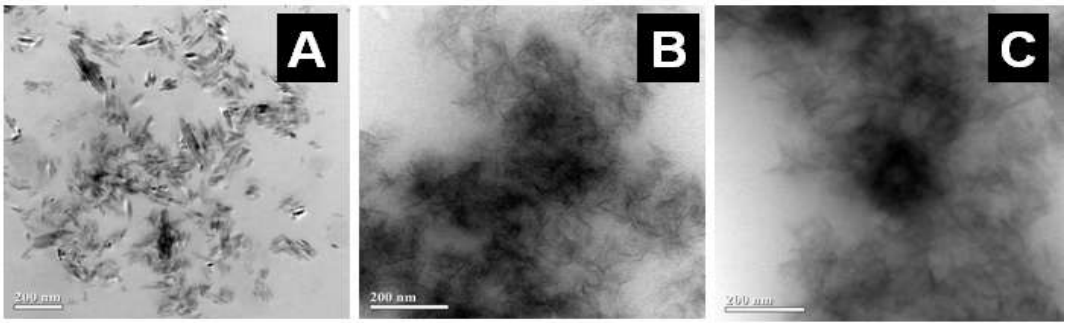

Figure 3.9 Transmission electron micrograph of colloidal $ZnCrO_4$ dispersions prepared in water/AOT/n-heptane W/O microemulsion. Scale bar: 200 nm. Concentration of $ZnCrO_4$ / m moldm^{-3}: A, 0.1; B, 0.3 and C, 0.7.

3.4. Summary and Conclusion

The $ZnCrO_4$ nanoparticles with controllable morphology can be synthesized in W/O microemulsion template under simple conditions. The synthesized $ZnCrO_4$ particle sizes were in a range of 100 to 200 nm, which is close to the border line dimensions between nano and micron scale. The $ZnCrO_4$ suspensions behaved like ordinary solutions obeying Beer's law with molar extinctions which strongly relies upon the water pool size (ω). The enthalpy of formation of the synthesized $ZnCrO_4$ obtained from ITC was exothermic with the non-linear dependence on ω. With an appropriate ω, the synthesized $ZnCrO_4$ nanoparticles exhibit good crystallinity with needle-like morphology as revealed by the XRD and TEM analyses. The band gap value was found to be 3.01 eV, which was comparable with many other synthesized nanomaterials.